Ocean Acoustic Propagation and Coherence Studies

Timothy F. Duda
Applied Ocean Physics and Engineering Department, MS 11
Woods Hole Oceanographic Institution, Woods Hole, MA 02543
phone: (508) 289-2495 fax: (508) 457-2194 email: tduda@whoi.edu

Award Number: N00014-14-1-0223

http://www.whoi.edu/people/tduda

LONG-TERM GOALS

The long-term objective is to develop knowledge of the factors controlling the mean and the variability of acoustic fields in the shallow ocean environment in the acoustic frequency band 50 Hz to 3000 Hz. Propagation variability is an inescapable complicating factor for both active and passive sonar systems, and for underwater acoustic communications. Reliable predictions of temporal and spatial variability of received underwater sound can improve processing and handling of signals of interest, for example the remediation of signal degradation, the exploitation of intermittent sonic information, or the exploitation of favorable propagation conditions.

OBJECTIVES

The main goal is to discover, analyze and describe mean properties of acoustic fields and time-varying acoustic effects caused by prominent deterministic propagation-altering events and phenomena. Example acoustic effects would be variation of horizontal coherence length, variation of signal level, variation of array gain (coherent spatial field summation), and properties of the (space- and time-dependent) spatial covariance matrices of acoustic fields. I plan to study specific acoustic effects caused by water-borne features that the community believes are the most influential: water-mass fronts, internal-wave packets, beam-like internal tides, and highly structured seafloors. These features can impart non-Gaussian form to the acoustic field variations that arise from ever-present stochastic features and may be Gaussian in the absence of the features but the presence of only Gaussian sound-speed variability. Seafloor features alone can also impart spatially non-Gaussian spatial field variation, with example features being sand ridges, slopes, valleys and canyons.

A secondary goal is to more fully describe the propagation-altering oceanic phenomena themselves. Working towards this goal is closely coupled with acoustics research, because we first need to know which features are the more relevant for acoustics, and to what detail we need to know them. This environmental research would be undertaken with acoustics as the main motivating factor.

APPROACH

Although much progress has been made in describing ocean acoustic variability, numerous factors motivate continued research, among them the high complexity of the ocean environment, the associated complexity of the propagated sound, and the lack of a simple conceptual framework for the

basic properties of shallow-water propagation regimes that depart from the most simple range-independent adiabatic mode situation. The research direction is toward such a framework, to be exploited in the use of underwater sound in shallow water. Our knowledge of acoustic field patterns in shallow water, building block towards a useful shallow-water acoustic framework, has made strong advances during the last 20 years through field studies and theoretical studies. We wish to continue this progression, establishing the relative real-world importance of various fluctuation-relevant ocean features, how the features interact, and how the sound behaves in the interacting features. In this approach, models of the environment are developed, through which sound propagation is simulated using both theoretical and purely computational methods, including our 3D parabolic equations solvers (Lin et al., 2013). The methodology includes building environmental models of hierarchical complexity, from which the salient acoustic processes and mechanisms can be identified and quantified.

The acoustic simulation tools and the environmental models are both key to the studies. The models of the variable waveguide features can be both idealized and realistic, with idealized models used to study parameter dependence and uncover basic physics, and realistic models used for comparing computed and/or theoretical results with experiment. Lying between these two activities is an implicit comparison of results from the idealized and realistic models, which may answer the question can insights obtained from the simple models be used to understand results that arise from the realistic models?

An insight that we have acquired this year is that it may be beneficial to examine the raw output of the models, for instance phasor behavior in time and space. Software that can objectively expose and categorize propagation behavior may also use be useful to construct, but simply looking directly at transient acoustic effects can be valuable, for instance as apparent in Badiey et al. (2005), Duda et al. (2012) and Badiey et al. (2014) where strong deterministic acoustic behaviors that are non-Gaussian (at least over the studied time intervals) are examined and explained.

The ocean models and the acoustic simulation tools will be run by the PI and by Arthur Newhall, in collaboration with other members of the WHOI Ocean Acoustics and Signals Laboratory. Five acoustic studies are planned:

1. Canyon and slope acoustics: Identify purely geometrically controlled (no ocean dynamics) vs. time-dependent acoustic field features and statistics
2. Rough-seafloor shelf acoustics: Determine whether findings concerning acoustic field complexity from water-column features are robust to bathymetric and sub-bottom uncertainty
3. Compare the roles of bathymetry fluctuations, sub-bottom properties variations, in the presence of internal waves
4. Comparison of simulated acoustic fields resulting from realistic ocean environment inputs and those resulting from idealized ocean environment inputs
5. Evaluate parameters associated with array signal processing and adaptive signal processing
6. Canyon or shallow-water experiment planning: (2015-16 for an anticipated 2017 or beyond experiment)

WORK COMPLETED

In Study 1, hierarchies of simulations are planned for a few bathymetric geometries, starting with a uniform sound speed in water above relief, adding refraction from background sound-speed profiles, adding spatially-dependent stratification, and finally temporally and spatially-dependent stratification. We have begun with the most complex. The 4D-varying ocean fields are taken from the S. Calif. Bight internal-tide response simulations (Ponte and Cornuelle, 2013). Simplifying the environment as planned to analyze complexity will be done sequentially.

Simulations of acoustic fields at 300 Hz in Coronado Canyon (Normark et al., 2009) have been added to the 700-Hz fields examined last year, The change gives broader area coverage (modeling capability scales with acoustic wavelength). Figure 1 shows bathymetry and output. Simulations are at one-hour intervals. The ocean structure contains mainly tidal frequency fluctuations, which are resolves at this sampling rate. Some flow energy may be present at higher harmonics of the tidal frequencies, as well as residual subtidal flows.

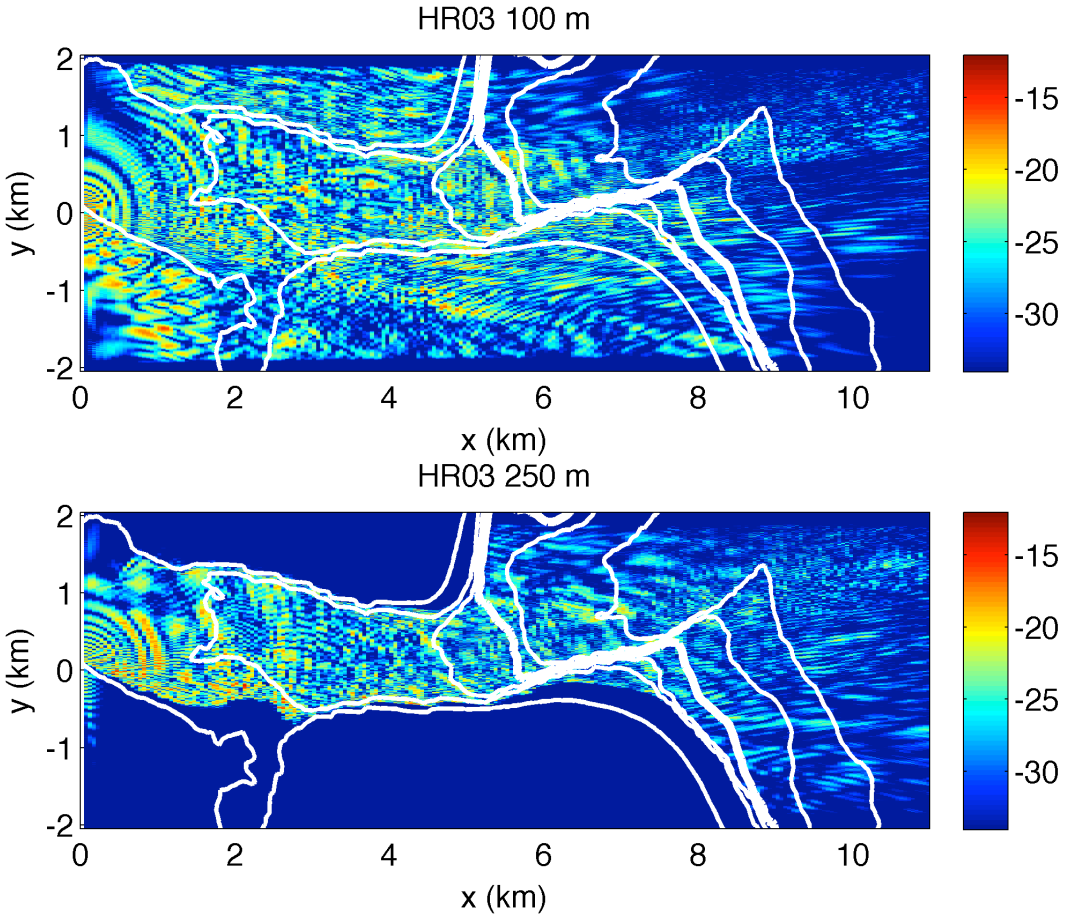

Figure 1: Snapshots of sound intensity (transmission loss, dB scale) at two depths for 3D parabolic equation-derived simulation outputs for 300-Hz sound going down Coronado Canyon from left to right are shown. The source is 40 m deep at [x,y]=[0,0]). White lines are depth contours with 100 m increment. The 500-m contour is thicker.

Statistics of the hourly 300-Hz outputs have been examined. As in our prior work, horizontal variability in the acoustic field $\Psi(x,y,z)$ was quantified in terms of the correlation function R_N

$$R_N(x) = \frac{\left\langle \Psi^*(x_0)\Psi(x_0+x)\right\rangle}{\left\langle \Psi(x_0)^2\right\rangle^{1/2}\left\langle \Psi(x_0+x)^2\right\rangle}$$

where the averaging (brackets) can be made by time averaging for stationary ergodic processes, and may include spatially averaging over x_0 for fields with homogeneous statistics (i.e. R_N is not a function of x_0, just as it as written). R_N was examined in detail by Duda et al. (2012) for field data from a place where internal wave effects were strong and the seabed was shallow and relatively flat. Note that $R_N(0)=1$. The point x = L where $R_N(L)$ = exp(-1) is referred to as the horizontal correlation length scale (or coherence length), L. The lagged product quantifies field variability, usually dominated by phase differences for typical ocean acoustic fields. The product behavior is linked to array gain for additive beamformer processors, which use sums of spatially lagged signals rather than the products. Gain and correlation can be expressed in terms of one another for certain functional forms of R_N (e.g. Cox, 1973). We have not proven it, but there is not likely to be a general relationship between the additive and multiplicative behaviors of fields with unconstrained R_N structure.

The field Ψ and the computation deserve some discussion. To analyze, we first beamform the signals, as was done with the SW06 data (Duda et al. 2012), eliminating phase wrap. Figure 2 shows beamformed output (100-m arrays) at two locations in the canyon area. This is an example of the near-raw output that we find useful to examine.

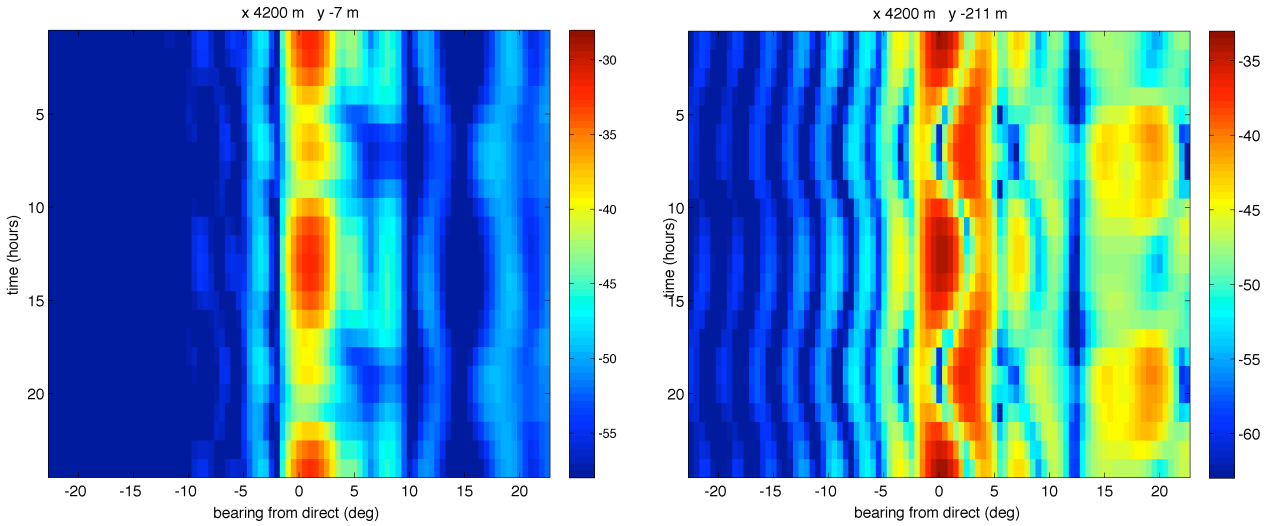

Figure 2: Beamformed (array-steered) output for two array locations at 60-m depth in the canyon are shown (level in dB). On the left an arrival from one direction, pulsating in time, is seen for a location along the centerline of the x,y calculation grid over the canyon,. On the right, output from a site close to the canyon edge shows multiple arrivals, one at high angle that pulsates and two or more interfering at small angle (directed at the source).

For a fluctuating process, the time mean is often subtracted from each point, and the residual forms the field to be analyzed. These fields can be analyzed to form the spatially-lagged covariance matrix (part of the spatiotemporal correlation matrix **R** for horizontal apertures, Johnson and Dudgeon, 1993). This matrix yields for example, the principal components (empirical orthogonal eigenfunctions) that efficiently describe the fluctuations. This would provide the spatial coherence behavior of the fluctuating field, but the mean values may need to be retained to make the best use of an extended array for detection or classification problems. We are working to examine relationships between principal component behavior, correlation behavior, and array gain behavior.

This suggests a second option where field-measured mean values, or mean values compared to an *a priori* model are used. A simple *a priori* model is the curved or spherical wavefront used for nearfield beamforming. A recent paper from our group studied apparent acoustic field decorrelation from ocean features such as front intervening between a sound source and an array location, which will impart an unknown but steady structure to Ψ (Lynch et al., 2014). If known, the feature and the structure could be accounted for to achieve gain over a very large array aperture (i.e. creating a very large effective L), but currently most ocean features are not well enough mapped to be accounted for, and actual L and effective L are both finite.

We continue to look into the implications of partial field coherence. The array gain AG for an N-element line array, the power of the beamformed signal divided by the power of the beamformed noise, divided the signal to noise ratio for a single sensor, is 10 $\log_{10}$ (N^2/N) for a perfectly coherent signal and incoherent noise. This can be written as AG = SNRarray/SNRsensor, where SNRsensor = Ssensor/Nsensor for a single sensor. For partial-array coherence, the coherence length can give AG for an arbitrarily long array by substituting $N + (L/\Delta y)^2 - (L/\Delta y)$ for N^2 in the numerator, where Δy is the inter-element spacing in meters, so that AG=10 $\log_{10}$ $(1+[(L/\Delta y)^2 - (L/\Delta y)]/N)$. The quantity $L/\Delta y$ is the number of effectively coherent sensors in the array. Noise is considered uncorrelated along the array in this model. This estimate of AG is useful because it may be able to distinquish between non-monotonic R_N behavior of multipath interference, and monotonically decreasing coherence, by comparison with direct AG computation. In log units, SNRarray = AG + Ssensor – Nsensor. SNRarray is tied closely to the detectability of a particular signal of interest. As long as AG + Ssensor exceeds Nsensor, the ambient noise level, the system is usable. Plots of results from this calculation are presented in the Results section.

RESULTS

Figure 3 plots correlation and array gain analysis for the 300-Hz canyon example of Figure 1. The correlation length scales at 60-m depth for signals steered toward the source with 100-m long synthetic arrays (34 elements) are shown. Also shown is signal excess Ssensor-Nsensor at all positions, again for 60-m depth, with source level 150 dB and Nsensor 95 dB. Lastly, a panel shows SNRarray with AG as in the model, from the depicted L.

The array gain can of course be computed directly from the simulation with standard delay and sum beamforming, to check whether the model that uses the behavior of the cross-product (the L estimate) to estimate AG is accurate. Agreement between the two would indicate that the R_N is generally monotonically decreasing and that the scale L gives usable array size. Figure 4 shows a good comparison along the line x = 7700 m, for 24 hours. A tidal frequency oscillation of AG is evident in the figure. The output of the beamforming is variable over time, but there are persistent patterns.

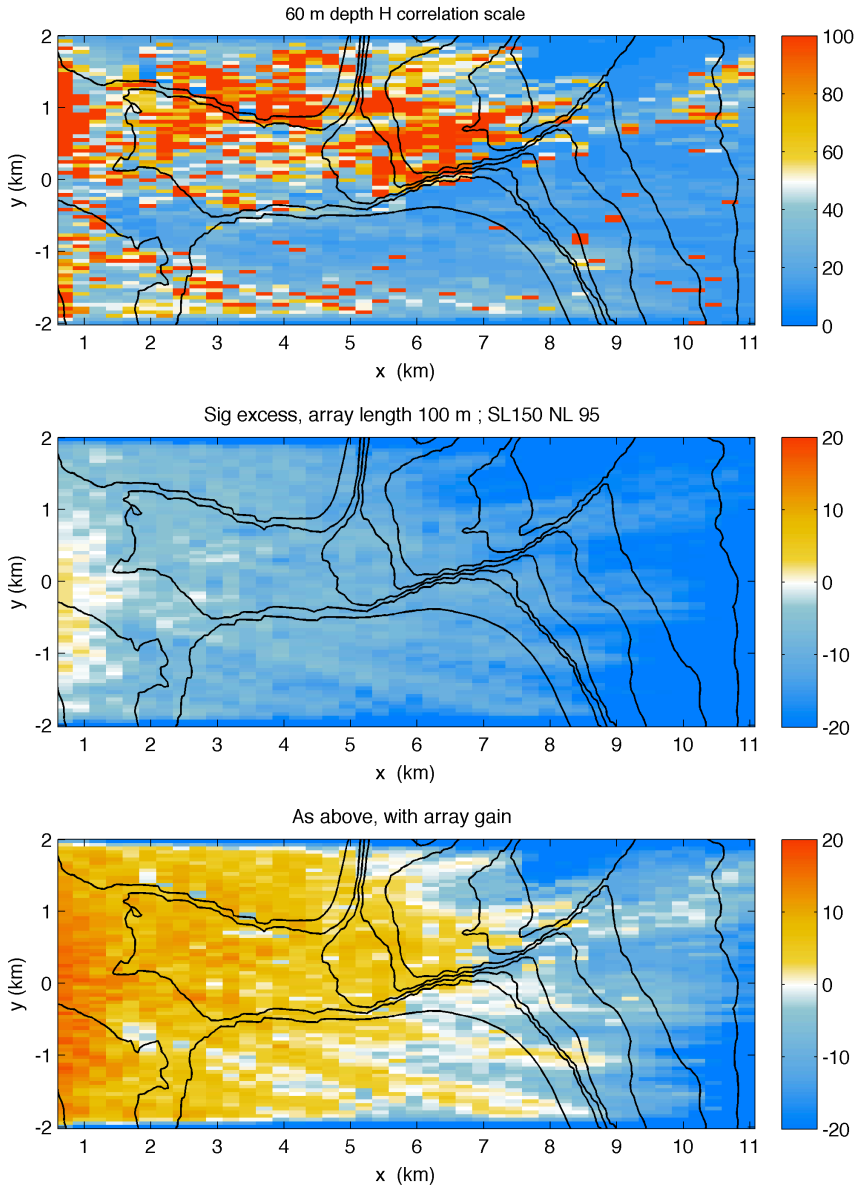

Figure 3: 3D parabolic equation-derived simulation outputs for 700-Hz sound going down Coronado Canyon from left to right (150 dB source is 40 m deep at the [x,y] origin. Black lines are depth contours as in Figure 1. The top shows the horizontal correlation length L for lag intervals in the y direction, calculated at 60 m depth, computed for beams directed at the source. The calculation is made with a 100-m aperture, so computed L cannot exceed 100 m. The center plot shows the average signal excess for sensors on the imaginary arrays with respect to a noise level of 95 dB. The lowest plot shows signal excess with respect to the same noise level after including estimated array gain as discussed in the text.

Figure 5 shows beamformer snapshots for two lines of array locations, again at 60-m depth, along with the 24-hr means of the outputs. The snapshots depart in detail from the mean (not yet quantified) but capture the major patterns of the signal directionality and strength.

The 24-hr time series along the 34-element arrays have been decomposed using principal component analysis (empirical modes). For the domain shown in Figure 3, the statistics of energy explained by

mode two (the 2nd most energetic) divided by the energy explained by mode one (most energetic) is quite variable. At 10% of the sites the ratio is greater than 0.27. At 2% the ratio is greater than .52. At 1% it is greater than 0.59. A single dominant mode would indicate that multipath arrivals fluctuate in unison; this might be expected for tidal effects on sound speed that are spatially coherent over the modeled domain. Departures from this are under examination. We are now looking into the correlation of significant multimode fluctuation and array gain performance. It is possible that they are independent. Preliminary analysis of related properties, direct-beam power versus mode-one fluctuation content, is shown in Figure 6. Single eof-mode fluctuation behavior is loosely tied to more power in the main arrival coming straight from the source at this range, (*x* of 7700 m).

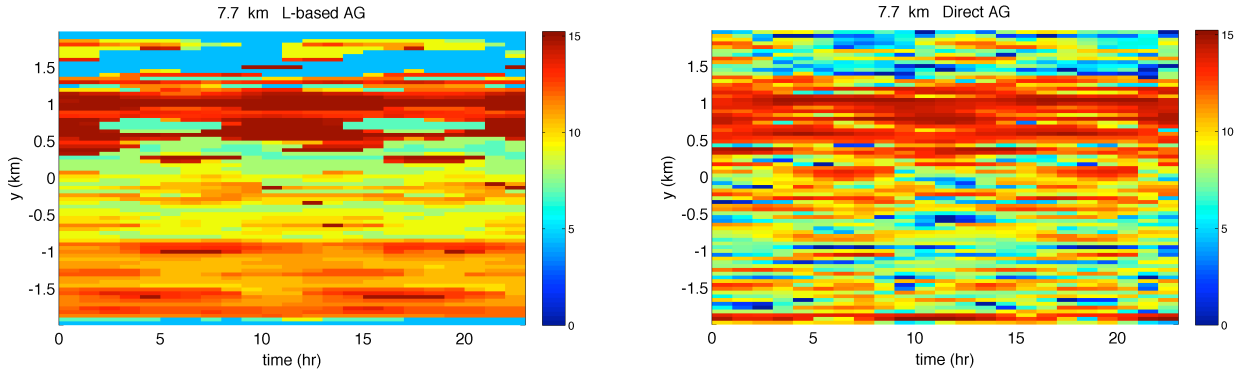

Figure 4: The L-based array gain estimate (left) which results from analysis of beamformed data snapshots, is compared to direct estimates of array gain made by summing the signals along arrays, after beamforming (right). Both calculations treat noise as uncorrelated between sensors. The computation is made hourly along a line in the y-direction at x = 7.7 km. Gain is higher over deep water, with the bathymetry plotted in Figure 3. Gain with full coherence of 34 elements is 15 dB

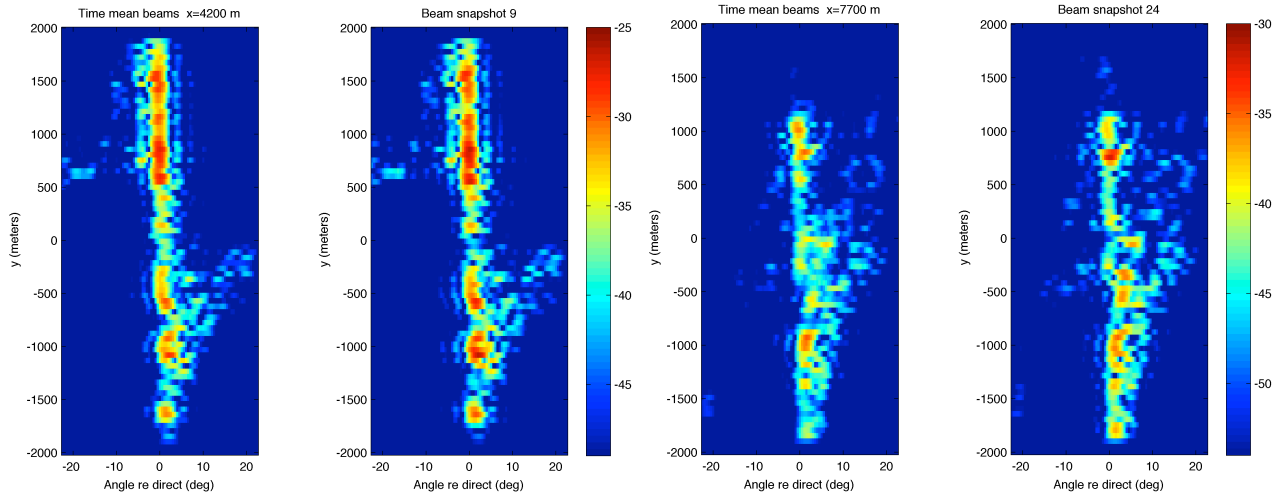

Figure 5: (left) 24-hour mean beamformer output is shown for a lien of arrays placed at x = 4200 m (see Figures 1 and 3). Zero degrees point at the source. So-called out-of-plane sound at higher angles is seen in the average, and is thus time-coherent. (2nd from left) One snapshot of the beamformer output is shown. The peak levels exceed the mean levels. (2nd from right) The 24-hour mean from the line at x = 7700 m is shown. The peak level is reduced at this range when compared to the closer range, and many locations show very little coherent arriving sound. (right) A snapshot at 7700 m range shows some transient arrivals that are not evident in the mean.

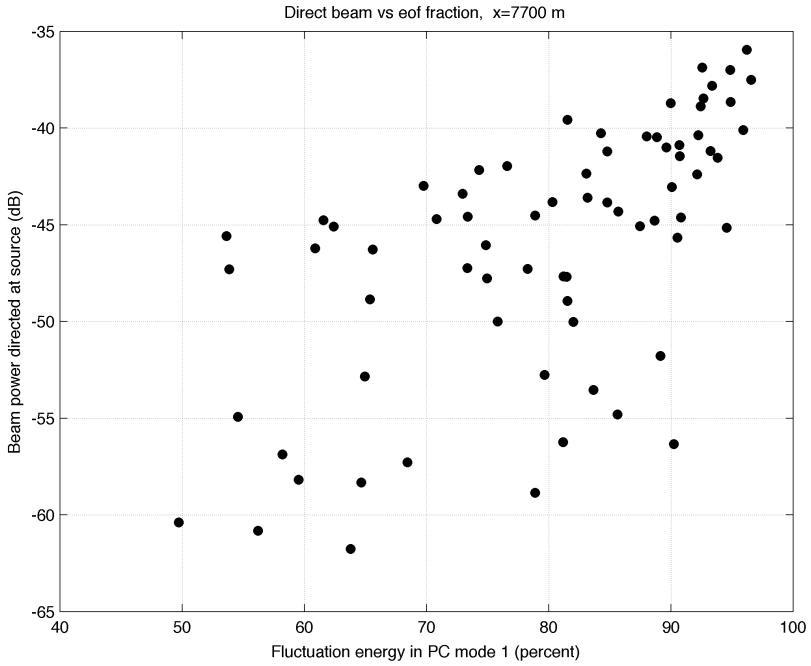

Figure 6: Direct-beam power (at the angle pointing from array to source) versus mode-one principal component fractional fluctuation energy, is shown.

IMPACT/APPLICATIONS

The ultimate performance limitations of marine acoustic systems are set by the properties of the sound signals that propagate within the fluctuating three-dimensional oceanic environment. Knowledge of the features that impact sound fields and how the features affect the sound can guide design and use of acoustic systems.

RELATED PROJECTS

The PI also has a MURI grant related managed by ONR. The project is working toward coupled modeling of the ocean environment and acoustics behavior within the environment. Information can be found at http://www.whoi.edu/sites/IODA. The PI also has a National Science Foundation physical Oceanography grant, with Co-PIs Y.-.T. Lin and Pierre Lermusiaux, to study ocean internal tide dynamics.

REFERENCES

Badiey, M., B. G. Katsnelson, J. F. Lynch, S. Pereselkov, and W. L. Siegmann, Measurement and modeling of three-dimensional sound intensity variations due to shallow-water internal waves, J. Acoust. Soc. Am., 117, 613-625, http://dx.doi.org/10.1121/1.1828571, 2005

Badiey, M., J. Eickmeier, and A. Song, Arrival-time fluctuations of coherent reflections from surface gravity water waves, J. Acoust. Soc. Am., 135, EL226-EL231, doi: 10.1121/1.4871577, 2014.

Cox, H., Line array performance when the signal coherence is spatially dependent, J. Acoust. Soc. Am., 54, 1743–1746, http://dx.doi.org/10.1121/1.1914473, 1973.

Duda, T. F., J. M. Collis, Y.-T. Lin, A. E. Newhall, J. F. Lynch and H. A. DeFerrari, Horizontal coherence of low-frequency fixed-path sound in a continental shelf region with internal wave activity, J. Acoust. Soc. Am., 131, 1782-1797, http://dx.doi.org/10.1121/1.3666003, 2012.

Gawarkiewicz, G., S. Jan, P. F. J. Lermusiaux, J. L. McClean, L. Centurioni, K. Taylor, B. Cornuelle, T. F. Duda, J. Wang, Y. J. Yang, T. Sanford, R.-C. Lien, C. Lee, M.-A. Lee, W. Leslie, P. J. Haley Jr., P. P. Niiler, G. Gopalakrishnan, P. Velez-Belchi, D.-K. Lee, and Y. Y. Kim, Circulation and intrusions northeast of Taiwan: Chasing and predicting uncertainty in the cold dome, Oceanography, 24, 110-121, http://dx.doi.org/10.5670/oceanog.2011.99, 2011.

Gawarkiewicz, G. and S. Jan, The Quantifying, Predicting, and Exploiting Uncertainty Program: Exploring oceanographic processes in a complex bathymetric shelf/slope environment affected by the Kuroshio, J. Mar. Res., 71, 1-18, http://dx.doi.org/10.1357/002224013807343443, 2013.

Johnson, D. H. and D. E. Dudgeon, *Array Signal Processing: Concepts and Techniques*, PTR Prentice-Hall Inc., Upper Saddle River, NJ, 1993.

Lin, Y.-T., T. F. Duda and A. E. Newhall, Three-dimensional sound propagation models using the parabolic-equation approximation and the split-step Fourier method, J. Comput. Acoust., 21, 1250018, http://dx.doi.org/10.1142/S0218396X1250018X, 2013.

Lynch, J. F., T. F. Duda and J. A. Colosi, Acoustical horizontal array coherence lengths and the "Carey Number", Acoustics Today, 10, 10-19, http://dx.doi.org/10.1121/1.4870172, 2014.

Newhall, A. E., G. G. Gawarkiewicz, J. F. Lynch, T. F. Duda, N. M. McPhee, F. B. Bahr, C. D. Marquette, Y.-T. Lin, S. Jan, J. Wang, C.-F. Chen, L. Y. S. Chiu, Y. J. Yang, R.-C. Wei, C. Emerson, D. Morton, T. Abbot, P. Abbot, B. Calder, L. Mayer, and P. F. J. Lermusiaux, Acoustics and oceanographic observations collected during the QPE Experiment by Research Vessels OR1, OR2 and OR3 in the East China Sea in the summer of 2009, WHOI Technical Report WHOI-2010-06, http://hdl.handle.net/1912/3914, 2010.

Normark, W. R., D. J. W. Piper, B. W. Romans, J. A. Covault, P. Darnell and R. W. Sliter, Submarine canyon and fan systems of the California Continental Borderland, The Geological Society of America, Special Paper 454, 2009.

Ponte, A. L., and Cornuelle, B. D., Coastal numerical modelling of tides: Sensitivity to domain size and remotely generated internal tide, Ocean Modelling, 62, 17-26, 10.1016/j.ocemod.2012.11.007, 2013.

PUBLICATIONS

Duda, T. F., W. G. Zhang, K. R. Helfrich, A. E. Newhall, Y.-T. Lin, and J. F. Lynch, Issues and progress in the prediction of ocean submesoscale features and internal waves, in Oceans '14 St. John's Conference Proceedings, IEEE/MTS, 2014. (9 pp.) [published, not refereed]

Lin, Y.-T., T. F. Duda, C. Emerson, G. Gawarkiewicz, A. E. Newhall, B. Calder, J. F. Lynch, P. Abbot, Y.-J. Yang and S. Jan, Experimental and numerical studies of sound propagation over a submarine canyon northeast of Taiwan, *IEEE J. Oceanic Eng., 40*, 237-149, http://dx.doi.org/10.1109/JOE.2013.2294291, 2014. [published, refereed]

Emerson, C., J. F. Lynch, P. Abbot, Y.-T. Lin, T. F. Duda, G. G. Gawarkiewicz, and C.-F. Chen, Acoustic propagation uncertainty and probabilistic prediction of sonar system performance in the southern East China Sea continental shelf and shelfbreak environments, *IEEE J. Oceanic Eng.,* http://dx.doi.org/10.1109/JOE.2014.2362820, 2015. [published online, refereed]

HONORS/AWARDS/PRIZES

Recipient: Timothy F. Duda, Woods Hole Oceanographic Institution
Award Name: Editors' Citation for Excellence in Refereeing - Journal of Geophysical Research Oceans (2014)
Award Sponsor: American Geophysical Union